http://dx.doi.org/10.5012/bkcs.2012.33.11.3777

A Series of 3D Lanthanide Complexes Containing (La(III), Sm(III) and Gd(III)) Metal-organic Frameworks: Synthesis, Structure, Characterization and Their Luminescent Properties

Huai-min Zhang, Hao Yang, Lan-zhi Wu, Shuang Song, and Li-rong Yang*

*Institute of Molecule and Crystal Engineering, College of Chemistry and Chemical Engineering, Henan University, Kaifeng 475004, P.R. China. *E-mail: lirongyang@henu.edu.cn*
Received July 16, 2012, Accepted August 28, 2012

Three kinds of 3D isomorphous and isostructural coordination polymers, namely, $\{[Ln_2(PDA)_3(H_2O)_3]\cdot 0.25H_2O\}_\infty$ (Ln = La(1), Sm(2), and Gd(3)) (PDA^{2-} = pyridine-2,6-dicarboxylate anion) have been synthesized under hydrothermal conditions and characterized by elemental analyses, IR spectroscopy, thermal analyses and single crystal X-ray diffraction. In these MOFs, Ln(III) centers adopt eight-coordinated and nine-coordinated with the N_1O_7 and N_2O_7 donor sets to construct distorted trianglar dodecahedron geometry and tricapped trigonal prism configurations, respectively. Based on the building block of tetranuclear homometallic $Ln_4C_4O_8$ unit (16-membered ring), 1-3 are connected into highly ordered 2D sheets *via* O-C-O linkers and further constructed into 3D architectures through hydrogen bonds. Crystallographic parameters suggest that the lanthanide contraction effect exist in these coordination polymers. Luminescent properties of the lanthanide-based MOFs (metal-organic frameworks) have been measured at room temperature, which reveal that they presenting ion-selective characters toward certain metals, such as Mg^{2+}, Cd^{2+} and Pb^{2+} ions.

Key Words : Synthesis, Structure, Isostructural, Metal-organic frameworks, Luminescent properties

Introduction

Recently, there has been substantial interest in the metal-organic frameworks (MOFs) based on lanthanide-containing coordination polymers due to the combination of inorganic and organic ligands may construct a large number of novel architectures,[1-8] and allows the rational design strategies to construct porous materials with high surface areas, predictable structures, and tunable pore sizes to target some specific functionalities,[9-12] which may potentially lead to industrial applications including gas storage and separation, catalysis, guest-exchange, molecular recognition, sensors and luminescent probes, *etc*.[13-29] Especially, in the lanthanide compounds, the f electrons exhibit highly localized and the emission behavior of the rare-earth ions, which make intriguing lanthanide MOFs remarkably suitable for the development of tunable luminescent sensors and probes for chemical species.[30-48] Such progress within this field prompts us to rationally design and fabricate lanthanide organic frameworks possessing functional sites for specific luminescent selectivity recognition and thus to tune their functional properties. Recently, many intriguing MOFs concerned with structures and luminescent properties have been reported.[49,50] Actually, owing to their hard character, Ln(III) ions show preference for hard binding sites having large electrostatic components so that anionic ligands such as carboxylates are strongly recommended, which may potentially provide various coordination modes and are in favor of the fabrication of higher-dimensional MOFs frameworks. Pyridine-2,6-dicarboxylic acid (H_2PDA) and its deprotonated anions ($HPDA^-$ and PDA^{2-} tuned under appropriate pH value) adopt flexible, multidentate coordination sites, and therefore may potentially provide various coordination modes which are in favor of the construction of higher-dimensional MOFs frameworks.[51-61] These organic fragments may adopt not only diverse coordination binding modes such as terminal monodentate, chelating to one metal center, bridging bidentate in *syn-syn*, *syn-anti*, or *anti-anti* conguration to metal centers, but also supramolecular contacts such as hydrogen bonding, π-π interactions, *etc*.[62]

Following our ongoing efforts toward the isolation of lanthanide MOFs,[63,64] here we wish to report a series of 3D lanthanide MOFs obtained from the self-assembly of bridging ligands pyridine-2,6-dicarboxylic acid and its deprotonated anions with lanthanide centers, leading to the formation of tetranuclear homometallic $Ln_4C_4O_8$ motifs which play the role of robust inorganic building blocks in the construction of the lanthanide MOFs. Thermal analyses prove that the skeletons of the title MOFs are stable under higher temperature. The emission spectra of the title MOFs at the presence of Mg^{2+}, Zn^{2+}, Cd^{2+}, Pb^{2+} Hg^{2+}, and Cu^{2+} are studied and compared with those of original MOFs. Some of the MOFs may be considered as luminescent probes toward certain metal ions.

Experimental

Reagents and General Techniques. All starting chemicals are analytical grade and used without further purification. Elemental analysis was performed with a Perkin-Elmer

240C elemental analyzer. Fourier transform infrared (FT-IR) were recorded with an AVATAR 360 FT-IR spectrometer (KBr pellets, in the region of 4000-400 cm^{-1}). The crystal structure was determined with a Bruker Smart CCD X-ray single-crystal diffractometer. Fluorescent data were collected with an F-7000 FL spectrophotometer at room temperature. Thermogravimetric (TG) and differential thermogravimetric (DTG) analyses were conducted with a Perkin-Elmer TGA7 system under flowing N_2 stream (flow rate 40 mL/min) from room temperature to 1000 °C at a heating rate of 10 K/min.

Hydrothermal Syntheses of the MOFs 1, 2 and 3. Synthesis of MOF **1**, **1** was synthesized from the reaction mixture of pyridine-2,6-dicarboxylic acid and lanthanum nitrate at a molar ratio of 5:3 in 10 mL distilled water. The resultant mixture was homogenized by stirring for 20 minutes at ambient temperature and then transferred into 20 mL Teflon-lined stainless steel autoclave under autogenous pressure at 160 °C for 3 days and then cooled to room temperature at a rate of 5 °C/h. After filtration, the product was washed with distilled water and then dried, and colorless transparent block crystals suitable for X-ray diffraction analysis were obtained. Elemental analysis calcd (%) for $C_{21}H_{15.50}N_3O_{15.25}La_2$: C, 30.33; H, 1.88; N, 5.05. Found: C, 30.41; H, 1.81; N, 5.09. IR data (KBr pellet, cm^{-1}): 3441 (br), 1615 (s), 1588 (s), 1567(s), 1443 (m), 1388 (m), 1276 (m), 1179 (w), 1077 (w), 1015 (w), 924 (w), 829 (w), 761 (m), 730 (m), 698 (w), 658 (m), 592 (w), 519 (w), 467 (w), 431 (w).

Synthesis of MOF **2**, **2** was synthesized by identical experimental procedures to that of **1** except that lanthanum nitrate was replaced by samarium nitrate. After filtration, the product was washed with distilled water and then dried and yellow block crystals suitable for X-ray diffraction analysis were finally isolated. Elemental analysis calcd (%) for $C_{21}H_{15.50}N_3O_{15.25}Sm_2$: C, 29.51; H, 1.83; N, 4.92. Found: C, 29.34; H, 1.96; N, 4.99. IR data (KBr pellet, cm^{-1}): 3413 (br), 1620 (s), 1592 (s), 1570 (s), 1457 (w), 1445 (s), 1394 (s), 1357 (m), 1293 (w), 1279 (m), 1195 (w), 1176 (w), 1076 (m), 1018 (m), 927 (w), 828 (w), 760 (w), 730 (s), 694 (m), 660 (m), 584 (w), 526 (w), 415 (w).

Synthesis of MOF **3**, **3** was synthesized using the same procedures for preparing **1** except that lanthanum nitrate was replaced by gadolinium nitrate. After filtration, the product was washed with distilled water and then dried and colorless transparent block crystals were isolated. Elemental analysis calcd (%) for $C_{21}H_{15.50}N_3O_{15.25}Gd_2$: C, 29.05; H, 1.80; N, 4.84. Found: C, 29.11; H, 1.86; N, 4.89. IR data (KBr pellet,

Table 1. Summary of crystallographic data for **1-3**

Data	**1**	**2**	**3**
CCDC deposit no.	831853	819230	831854
Empirical formula	$C_{21}H_{15.50}N_3O_{15.25}La_2$	$C_{21}H_{15.50}N_3O_{15.25}Sm_2$	$C_{21}H_{15.50}N_3O_{15.25}Gd_2$
Formula weight	831.68	854.56	868.36
Temperature/K	296(2)	296(2)	296(2)
Wavelength/Å	0.71073	0.71073	0.71073
Crystal system	monoclinic	monoclinic	monoclinic
space group	$P\,2_1/c$	$P\,2_1/c$	$P\,2_1/c$
a / Å	11.045(5)	10.9501(7)	10.9245(7)
b / Å	17.612(8)	17.4746(11)	17.4705(12)
c / Å	13.665(6)	13.2811(8)	13.2092(9)
α / (°)	90	90	90
β / (°)	100.325(7)	101.4440(10)	101.6310(10)
γ / (°)	90	90	90
Z	4	4	4
Density(calculated)	2.112 gcm^{-3}	2.279 gcm^{-3}	2.336 gcm^{-3}
F(000)	1594	1634	1650
Crystal size / mm^3	0.22 × 0.16 × 0.13	0.33 × 0.17 × 0.11	0.48 × 0.38 × 0.26
θ range for data collection / (°)	1.87 to 25.00	1.90 to 25.00	1.90 to 25.00
Limiting indices	$-11 \le h \le 13$, $-12 \le k \le 20$, $-16 \le l \le 16$	$-13 \le h \le 12$, $-20 \le k \le 20$, $-15 \le l \le 15$	$-12 \le h \le 12$, $-20 \le k \le 20$, $-15 \le l \le 9$
Reflections collected / unique	12488/4589 [R_{int} = 0.0743]	12581/4397 [R_{int} = 0.0227]	12359/4349 [R_{int} = 0.0223]
Refinement method	Full-matrix least- squares on F^2		
Data / restraints / parameters	4589 / 6 / 379	4379 / 6 / 379	4349 / 0 / 380
Goodness-of-fit on F^2	0.945	1.182	1.081
Volume / $Å^3$	2615(2)	2490.8(3)	2469.3(3)
Final R indices [$I > 2\sigma(I)$]	R_1 = 0.0399, wR_2 = 0.0925	R_1 = 0.0260, wR_2 = 0.0526	R_1 = 0.0198, wR_2 = 0.0507
R indices (all data)	R_1 = 0.0468, wR_2 = 0.0944	R_1 = 0.0298, wR_2 = 0.0538	R_1 = 0.0219, wR_2 = 0.0515
Largest diff. peak and hole/($e \cdot Å^{-3}$)	0.929 and -1.263	0.705 and -0.820	1.063 and -0.586

cm^{-1}): 3409 (br), 1616 (s), 1571 (s), 1458 (m), 1447 (m), 1396 (m), 1359 (w), 1295 (w), 1280 (m), 1176 (w), 1019 (w), 928 (w), 828 (w), 760 (m), 730 (m), 694 (w), 661 (w), 586 (w), 472 (w) , 437 (w), 417 (w).

X-Ray Crystallographic Determination. Single-crystal X-ray diffraction measurements of MOFs **1**, **2** and **3** were carried out on a Bruker Smart CCD X-ray single-crystal diffractometer. Reflection data were measured at 296(2) K using graphite monochromated MoKα-radiation (λ = 0.71073 Å) and ω-scan technique. All independent reflections were collected in a range of 1.87 to 25.00°, 1.88 to 25.00°, 1.90 to 25.00° and 1.90 to 25.00° for MOFs **1**, **2** and **3**, respectively, and determined in the subsequent refinement. SADABS Multi-scan empirical absorption corrections were applied to the data processing.[65] The crystal structures were solved by direct methods and Fourier synthesis. Positional and thermal parameters were refined by the full-matrix least-squares method on F^2 using the SHELXTL software package.[66] Anisotropic thermal parameters were assigned to all non-hydrogen atoms. The hydrogen atoms were set in calculated positions and refined as riding atoms with a common fixed isotropic thermal parameter. Analytical expressions of neutral-atom scattering factors were employed, and anomalous dispersion corrections were incorporated. The crystallographic data, selected bond lengths and angles for MOFs **1**, **2** and **3** are listed in Table 1, Table 2 and Table 3, respectively.

Each structure deposited will be given a deposition number (CCDC), and the number should be supplied at the Experimental section with the following standard text: Crystallographic data for the structures reported here have been deposited with CCDC (Deposition No. CCDC-831853, 819230, 831854). These data can be obtained free of charge *via* http://www.ccdc.cam.ac.uk/conts/retrieving.html or from CCDC, 12 Union Road, Cambridge CB2 1EZ, UK, E-mail: deposit@ccdc.cam.ac.uk

Results and Discussion

The IR Spectra of the MOFs. MOFs **1**, **2** and **3** are insoluble in common solvents such as CH_3COCH_3, CH_3CH_2OH, CH_3CN and THF, but soluble in CH_3OH or DMF. The structures of the MOFs are identied by satisfactory elemental analysis, IR and X-ray diffraction. High yield of the products indicate that the title MOFs are thermodynamically stable under the reaction conditions. The IR spectra of the three compounds are similar. The strong and broad absorption bands in the ranges of 3441-3409 cm^{-1} and 924-928 cm^{-1} in **1**, **2** and **3** are assigned to the characteristic peaks of water

Table 2. Selected bond lengths (Å) for **1-3**

Bond lengths					
MOF **1**[a]					
La(1)-O(12)	2.409(5)	La(1)-O(2W)	2.605(4)	La(2)-O(2)	2.588(5)
La(1)-O(4)	2.421(4)	La(1)-N(3)	2.651(5)	La(2)-O(2)$^{\#1}$	2.622(4)
La(1)-O(8)	2.439(5)	La(2)-O(9)	2.500(4)	La(2)-O(1W)	2.640(5)
La(1)-O(11)	2.523(5)	La(2)-O(6)	2.517(5)	La(2)-N(2)	2.664(5)
La(1)-O(3W)	2.528(6)	La(2)-O(3)	2.534(5)	La(2)-N(1)	2.704(5)
La(1)-O(10)	2.570(5)	La(2)-O(7)	2.580(4)		
Interation of metal-metal (Å)					
La(1)···La(2)	6.619(2)	La(2)···La(2A)	4.448(2)		
MOF **2**[b]					
Sm(1)-O(2)	2.416(3)	Sm(1)-O(6)	2.544(3)	Sm(2)-O(10)	2.429(3)
Sm(1)-O(12)	2.420(3)	Sm(1)-N(1)	2.562(3)	Sm(2)-O(3W)	2.451(3)
Sm(1)-O(7)	2.448(3)	Sm(1)-N(2)	2.592(3)	Sm(2)-O(11)	2.507(3)
Sm(1)-O(3)	2.512(3)	Sm(2)-O(9)	2.303(3)	Sm(2)-O(2W)	2.507(3)
Sm(1)-O(6)$^{\#1}$	2.536(3)	Sm(2)-O(8)	2.323(3)	Sm(2)-N(3)	2.543(3)
Sm(1)-O(1W)	2.543(3)	Sm(2)-O(4)	2.350(3)		
Interation of metal-metal (Å)					
Sm(1)···Sm(2)	6.488(4)	Sm(2)···Sm(2A)	4.295(3)		
MOF **3**[c]					
Gd(1)-O(9)	2.396(2)	Gd(1)-O(6)	2.535(3)	Gd(2)-O(11)	2.412(3)
Gd(1)-O(2)	2.401(3)	Gd(1)-N(1)	2.536(3)	Gd(2)-O(3W)	2.438(3)
Gd(1)-O(7)	2.431(2)	Gd(1)-N(2)	2.567(3)	Gd(2)-O(10)	2.489(2)
Gd(1)-O(3)	2.496(2)	Gd(2)-O(12)	2.286(3)	Gd(2)-O(2W)	2.499(3)
Gd(1)-O(1W)	2.514(3)	Gd(2)-O(8)	2.300(3)	Gd(2)-N(3)	2.511(3)
Gd(1)-O(6)$^{\#1}$	2.515(2)	Gd(2)-O(4)	2.329(3)		
Interation of metal-metal (Å)					
Gd(1)···Gd(2)	6.463(4)	Gd(2)···Gd(2A)	4.268(3)		

[a]Symmetry transformations used to generate equivalent atoms: $^{\#1}$–x+1, –y+1, –z+1. [b]Symmetry transformations used to generate equivalent atoms: $^{\#1}$–x, –y, –z+1. [c]Symmetry transformations used to generate equivalent atoms: $^{\#1}$–x+2, –y, –z+1.

Table 3. Selected bond angles (deg) for **1-3**

Bond angles					
MOF **1**[a]					
O(12)-La(1)-O(4)	100.17(19)	O(4)-La(1)-N(3)	78.25(16)	O(9)-La(2)-O(1W)	70.94(14)
O(12)-La(1)-O(8)	86.06(19)	O(8)-La(1)-N(3)	78.58(17)	O(6)-La(2)-O(1W)	76.40(15)
O(4)-La(1)-O(8)	153.30(18)	O(11)-La(1)-N(3)	61.39(15)	O(3)-La(2)-O(1W)	141.34(15)
O(12)-La(1)-O(11)	163.63(18)	O(3W)-La(1)-N(3)	125.99(19)	O(7)-La(2)-O(1W)	136.30(14)
O(4)-La(1)-O(11)	90.51(17)	O(10)-La(1)-N(3)	61.06(15)	O(2)-La(2)-O(1W)	80.58(14)
O(8)-La(1)-O(11)	89.93(17)	O(2W)-La(1)-N(3)	139.09(14)	O(2)$^{\#1}$-La(2)-O(1W)	67.08(14)
O(12)-La(1)-O(3W)	89.3(2)	O(9)-La(2)-O(6)	87.76(15)	O(9)-La(2)-N(2)	141.46(15)
O(4)-La(1)-O(3W)	133.88(18)	O(9)-La(2)-O(3)	79.40(15)	O(6)-La(2)-N(2)	61.28(15)
O(8)-La(1)-O(3W)	71.58(19)	O(6)-La(2)-O(3)	78.24(15)	O(3)-La(2)-N(2)	72.58(15)
O(11)-La(1)-O(3W)	74.42(19)	O(9)-La(2)-O(7)	140.55(14)	O(7)-La(2)-N(2)	60.85(15)
O(12)-La(1)-O(10)	72.33(17)	O(6)-La(2)-O(7)	122.04(14)	O(2)-La(2)-N(2)	134.33(15)
O(4)-La(1)-O(10)	78.19(15)	O(3)-La(2)-O(7)	82.17(16)	O(2)$^{\#1}$-La(2)-N(2)	85.46(15)
O(8)-La(1)-O(10)	79.11(17)	O(9)-La(2)-O(2)	82.78(14)	O(1W)-La(2)-N(2)	117.93(15)
O(11)-La(1)-O(10)	122.45(15)	O(6)-La(2)-O(2)	156.89(15)	O(9)-La(2)-N(1)	69.92(15)
O(3W)-La(1)-O(10)	146.36(17)	O(3)-La(2)-O(2)	120.23(14)	O(6)-La(2)-N(1)	135.80(15)
O(12)-La(1)-O(2W)	78.26(17)	O(7)-La(2)-O(2)	76.92(14)	O(3)-La(2)-N(1)	60.83(16)
O(4)-La(1)-O(2W)	69.05(15)	O(9)-La(2)-O(2)$^{\#1}$	128.73(14)	O(7)-La(2)-N(1)	70.63(15)
O(8)-La(1)-O(2W)	137.49(16)	O(6)-La(2)-O(2)$^{\#1}$	109.02(14)	O(2)-La(2)-N(1)	59.44(15)
O(11)-La(1)-O(2W)	94.28(15)	O(3)-La(2)-O(2)$^{\#1}$	150.15(15)	O(2)$^{\#1}$-La(2)-N(1)	114.75(15)
O(3W)-La(1)-O(2W)	68.99(17)	O(7)-La(2)-O(2)$^{\#1}$	69.35(14)	O(1W)-La(2)-N(1)	126.33(15)
O(10)-La(1)-O(2W)	130.69(15)	O(2)-La(2)-O(2)$^{\#1}$	62.75(16)	N(2)-La(2)-N(1)	115.63(17)
O(12)-La(1)-N(3)	132.78(17)				
MOF **2**[b]					
O(2)-Sm(1)-O(12)	83.77(10)	O(12)-Sm(1)-N(1)	140.22(10)	O(8)-Sm(2)-O(3W)	134.01(11)
O(2)-Sm(1)-O(7)	76.73(10)	O(7)-Sm(1)-N(1)	72.51(10)	O(4)-Sm(2)-O(3W)	72.81(12)
O(12)-Sm(1)-O(7)	78.71(10)	O(3)-Sm(1)-N(1)	62.39(10)	O(10)-Sm(2)-O(3W)	71.84(12)
O(2)-Sm(1)-O(3)	125.74(10)	O(6)$^{\#1}$-Sm(1)-N(1)	82.44(10)	O(9)-Sm(2)-O(11)	73.07(11)
O(12)-Sm(1)-O(3)	141.07(10)	O(1W)-Sm(1)-N(1)	114.82(10)	O(8)-Sm(2)-O(11)	78.72(11)
O(7)-Sm(1)-O(3)	84.05(10)	O(6)-Sm(1)-N(1)	134.22(10)	O(4)-Sm(2)-O(11)	76.71(11)
O(2)-Sm(1)-O(6)$^{\#1}$	106.07(10)	O(2)-Sm(1)-N(2)	135.01(11)	O(10)-Sm(2)-O(11)	126.13(10)
O(12)-Sm(1)-O(6)$^{\#1}$	130.64(9)	O(12)-Sm(1)-N(2)	70.29(10)	O(3W)-Sm(2)-O(11)	145.90(12)
O(7)-Sm(1)-O(6)$^{\#1}$	150.48(10)	O(7)-Sm(1)-N(2)	62.83(10)	O(9)-Sm(2)-O(2W)	77.64(11)
O(3)-Sm(1)-O(6)$^{\#1}$	70.38(9)	O(3)-Sm(1)-N(2)	70.79(10)	O(8)-Sm(2)-O(2W)	69.18(10)
O(2)-Sm(1)-O(1W)	71.69(10)	O(6)$^{\#1}$-Sm(1)-N(2)	118.79(10)	O(4)-Sm(2)-O(2W)	137.92(11)
O(12)-Sm(1)-O(1W)	71.07(10)	O(1W)-Sm(1)-N(2)	128.07(10)	O(10)-Sm(2)-O(2W)	90.42(11)
O(7)-Sm(1)-O(1W)	138.00(10)	O(6)-Sm(1)-N(2)	61.69(10)	O(3W)-Sm(2)-O(2W)	69.23(11)
O(3)-Sm(1)-O(1W)	137.23(10)	N(1)-Sm(1)-N(2)	117.10(11)	O(11)-Sm(2)-O(2W)	131.07(10)
O(6)$^{\#1}$1-Sm(1)-O(1W)	67.06(9)	O(9)-Sm(2)-O(8)	100.62(13)	O(9)-Sm(2)-N(3)	135.15(11)
O(2)-Sm(1)-O(6)	153.17(10)	O(9)-Sm(2)-O(4)	84.20(13)	O(8)-Sm(2)-N(3)	77.48(11)
O(12)-Sm(1)-O(6)	84.89(9)	O(8)-Sm(2)-O(4)	152.35(12)	O(4)-Sm(2)-N(3)	80.05(12)
O(7)-Sm(1)-O(6)	124.49(10)	O(9)-Sm(2)-O(10)	160.02(11)	O(10)-Sm(2)-N(3)	63.61(10)
O(3)-Sm(1)-O(6)	76.59(9)	O(8)-Sm(2)-O(10)	89.74(11)	O(3W)-Sm(2)-N(3)	124.98(12)
O(6)$^{\#1}$-Sm(1)-O(6)	64.54(11)	O(4)-Sm(2)-O(10)	94.55(12)	O(11)-Sm(2)-N(3)	62.53(10)
O(1W)-Sm(1)-O(6)	81.65(9)	O(9)-Sm(2)-O(3W)	88.85(13)	O(2W)-Sm(2)-N(3)	137.70(11)
O(2)-Sm(1)-N(1)	63.49(10)				
MOF **3**[c]					
O(9)-Gd(1)-O(2)	83.25(9)	O(2)-Gd(1)-N(1)	63.86(9)	O(8)-Gd(2)-O(3W)	134.02(10)
O(9)-Gd(1)-O(7)	78.46(8)	O(7)-Gd(1)-N(1)	72.34(9)	O(4)-Gd(2)-O(3W)	73.18(10)
O(2)-Gd(1)-O(7)	76.67(9)	O(3)-Gd(1)-N(1)	62.77(9)	O(11)-Gd(2)-O(3W)	71.37(10)
O(9)-Gd(1)-O(3)	140.83(8)	O(1W)-Gd(1)-N(1)	114.29(9)	O(12)-Gd(2)-O(10)	73.31(9)
O(2)-Gd(1)-O(3)	126.49(8)	O(6)$^{\#1}$-Gd(1)-N(1)	82.17(9)	O(8)-Gd(2)-O(10)	78.82(9)
O(7)-Gd(1)-O(3)	84.28(9)	O(6)-Gd(1)-N(1)	134.32(9)	O(4)-Gd(2)-O(10)	76.26(9)
O(9)-Gd(1)-O(1W)	71.32(8)	O(9)-Gd(1)-N(2)	70.11(9)	O(11)-Gd(2)-O(10)	127.32(8)

Table 3. Continued

Bond angles					
O(2)-Gd(1)-O(1W)	70.66(8)	O(2)-Gd(1)-N(2)	135.11(9)	O(3W)-Gd(2)-O(10)	145.72(10)
O(7)-Gd(1)-O(1W)	137.40(8)	O(7)-Gd(1)-N(2)	63.30(9)	O(12)-Gd(2)-O(2W)	77.50(10)
O(3)-Gd(1)-O(1W)	137.47(8)	O(3)-Gd(1)-N(2)	70.72(8)	O(8)-Gd(2)-O(2W)	69.01(9)
O(9)-Gd(1)-O(6)$^{\#1}$	130.98(8)	O(1W)-Gd(1)-N(2)	128.31(9)	O(4)-Gd(2)-O(2W)	138.35(10)
O(2)-Gd(1)-O(6)$^{\#1}$	105.47(8)	O(6)$^{\#1}$-Gd(1)-N(2)	119.33(9)	O(11)-Gd(2)-O(2W)	89.26(9)
O(7)-Gd(1)-O(6)$^{\#1}$	150.49(8)	O(6)-Gd(1)-N(2)	62.14(8)	O(3W)-Gd(2)-O(2W)	69.33(9)
O(3)-Gd(1)-O(6)$^{\#1}$	70.71(8)	N(1)-Gd(1)-N(2)	117.40(9)	O(10)-Gd(2)-O(2W)	130.95(9)
O(1W)-Gd(1)-O(6)$^{\#1}$	66.98(8)	O(12)-Gd(2)-O(8)	100.87(11)	O(12)-Gd(2)-N(3)	136.17(10)
O(9)-Gd(1)-O(6)	85.21(8)	O(12)-Gd(2)-O(4)	84.00(11)	O(8)-Gd(2)-N(3)	77.26(10)
O(2)-Gd(1)-O(6)	152.20(9)	O(8)-Gd(2)-O(4)	152.02(10)	O(4)-Gd(2)-N(3)	80.31(10)
O(7)-Gd(1)-O(6)	125.41(8)	O(12)-Gd(2)-O(11)	158.75(9)	O(11)-Gd(2)-N(3)	64.03(9)
O(3)-Gd(1)-O(6)	76.62(8)	O(8)-Gd(2)-O(11)	89.52(10)	O(3W)-Gd(2)-N(3)	124.81(10)
O(1W)-Gd(1)-O(6)	81.69(8)	O(4)-Gd(2)-O(11)	95.53(10)	O(10)-Gd(2)-N(3)	63.29(9)
O(6)$^{\#1}$-Gd(1)-O(6)	64.61(9)	O(12)-Gd(2)-O(3W)	88.30(11)	O(2W)-Gd(2)-N(3)	136.99(9)
O(9)-Gd(1)-N(1)	139.88(9)				

[a]Symmetry transformations used to generate equivalent atoms: $^{\#1}$–x+1, –y+1, –z+1. [b]Symmetry transformations used to generate equivalent atoms: $^{\#1}$–x, –y, –z+1. [c]Symmetry transformations used to generate equivalent atoms: $^{\#1}$–x+2, –y, –z+1.

molecules in coordination and lattice forms.[67-69] The strong vibrations appeared at about 1615 cm^{-1} and 1360 cm^{-1} in **1-3** are ascribed to the coordinated carboxylates. The $\delta_{O\text{-}C\text{-}O}$ vibration in plane occurs in sharp peaks in the range of 660-760 cm^{-1}. The absorption at about 1570 cm^{-1} is related to the NH stretching vibration.[70] The absence of the characteristic bands ranging from1690 to 1730 cm^{-1} indicates that the H_2PDA ligands are completely deprotonated in the form of PDA^{2-} anions upon reaction with the metal ions.[71,72] The same conclusions are also supported by the results obtained from X-ray diffraction measurements.

Structural Description of the MOFs. The single-crystal analyses reveal that **1-3** are isomorphous and isostructural, crystallizing in monoclinic space group *P*2(1)/*c*. Here, MOF **2**, $\{[Sm_2(PDA)_3(H_2O)_3]\cdot 0.25H_2O\}_\infty$, is selected as an example to describe the formation of 3D framework in detail. The coordination environment of Sm(III) centers with the coordination modes of the PDA^{2-} ligands in MOF **2** is shown in Figure 1(a) where samarium entities are connected with carboxylic oxygen atoms in two types of coordination environments. Namely, Sm(1) is nine-coordinated with the N_2O_7 donor set containing one O atom deriving from one molecule of terminal water and the rest coordination atoms deriving from PDA^{2-} ligands, while Sm(2) is eight-coordinated with the N_1O_7 donor set containing two O atoms coming from two molecules of terminal water. Besides, Sm(1) ion shows tricapped trigonal prism configurations, whereas Sm(2) ion in the asymmetric coordination unit of **2** presents distorted triangular dodecahedral geometry (as illustrated in Figure 1(b, c)). There exist three kinds of coordination modes *a*, *b* and *c* in the structure, around Sm(1) ion, there are four PDA^{2-} anions: one adopts tetradentate *a* mode, one adopts pentadentate *b* mode, and two adopt pentadentate *c* mode; whereas four PDA^{2-} anions surround Sm(2) ion *via* two molecules of PDA^{2-} in *a* mode, one molecule of PDA^{2-} in *b* mode and one in *c* mode (see Scheme 1). The Sm–O_{PDA} distances range from 2.303(3) to 2.544(3) Å, those of La–O_W are between 2.451(3) and 2.543(3) Å; and the average Sm–O_{PDA} bond length is significantly shorter than that of La–O_W bonds.. The Sm–N distances are in the range of 2.543(3)-2.592(3) Å. The bond length data in the present work are consistent with those in previous work covering lanthanide coordination polymers.[73-78]

In the framework, Sm(1) and Sm(2) are connected through carboxylic oxygen bridges (O(7)–C(14)–O(8)) from one

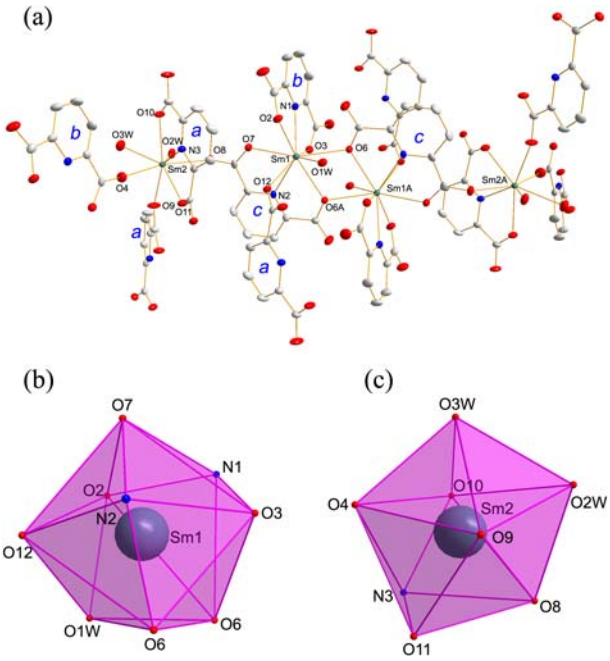

Figure 1. (a) Coordination environment of **2** with thermal ellipsoids at 30% probability; the asymmetric unit and the related coordination atoms are labeled; lattice water and hydrogen atoms are omitted for clarity. (b) and (c) Highlight of the coordination polyhedra for the two crystallographically independent Sm(III) ions. Cyan, Sm; blue, N; red, O; gray, C.

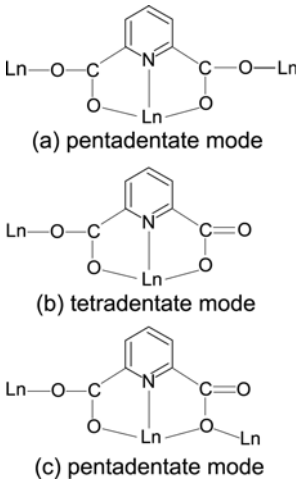

Scheme 1. Typical coordination modes of the PDA^{2-} anions in the MOFs.

PDA^{2-} ligand in *c* mode (μ_3-(η^3-N,O,O'), O'',O''' fashion), while Sm(1) and Sm(1A) are connected through two carboxylic oxygen bridges (O(6), O(6A)) from two PDA^{2-} ligands in *c* mode to form an approximate rhombus Sm_2O_2 grid (Sm(1)-O(6)-Sm(1A)-O(6A)-Sm(1)) with diagonal angles of 64.552(9)° (∠O(6)-Sm(1)-O(6A) and ∠O(6)-Sm(1A)-O(6A)) and 115.478(1)° (∠Sm(1)-O(6)-Sm(1A) and ∠Sm(2)-O(6A)-Sm(1A)), respectively. The four Sm(III) ions are well-separated, with the nonbonding distances of Sm(1)···Sm(2) and Sm(1)···Sm(1A) being 6.488(4) and 4.295(3) Å, respectively, which suggests that the double-oxygen-bridge linkage of Sm(1)···Sm(1A) is much more stronger than the O–C–O bridging linkage in Sm(1)···Sm(2).

The modular MOF 2 is built upon the building block of tetranuclear homometallic $Sm_4C_4O_8$ unit (16-membered ring with the dimension of 12.259(6) × 4.295(3) Å linked through carboxylic oxygen atoms) whose neighboring Sm(III) ions are bridged by O–C–O groups in μ_2-(η^1-O),(η^1-O') fashion and Sm(1) and Sm(1A) are bridged by O(6) and O(6A) in μ_2-(η^1-O),(η^1-O') fashion, as illustrated in Figure 2. The adjacent $Sm_4C_4O_8$ units are connected by two carboxyl bridges (O–C–O) in μ_2-(η^1-O),(η^1-O') fashion to propagate an infinite 1D chain and the adjacent chains are connected *via* carboxyl bridges (O–C–O) to form a 2D corrugated layer (see Figure 3). The 2D corrugated sheet is further assembled up and down through hydrogen bonds among coordinated carboxyl oxygen atoms (O(1), O(3), O(5), O(11)) and water molecules (O(1W), O(2W), O(3W) and O(4W)) to construct a 3D architecture (see Figure 4). The parameters of hydrogen bonds are listed in Table 4.

Lanthanide Contraction. MOFs **1-3** are isomorphous and isostructural, as above mentioned. Corresponding crystal lattice constants of these MOFs clearly exhibit the lanthanide contraction effect. As shown in Table 5, the average distances of Ln–O_W, Ln–O_C, Ln–N and Ln···Ln in **1-3** decrease regularly with the series of La, Sm to Gd, where it was ascribed to crystal field contractions of those rare earth ions lacking spherical symmetry.[79,80] The 4f electrons are shielded by the $5s^2$ and $5p^6$ orbitals and for the MOFs they are scarcely available for covalent interaction with the ligands. Hence interactions are largely of electrostatic nature and the geometries of the Ln(III) MOFs are determined by steric factors rather than electronic ones.[49]

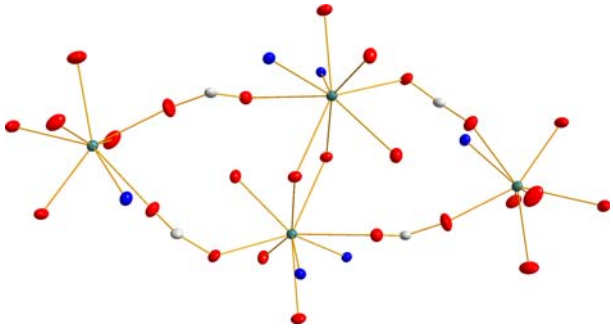

Figure 2. $Sm_4C_4O_8$ building block of MOF **2**.

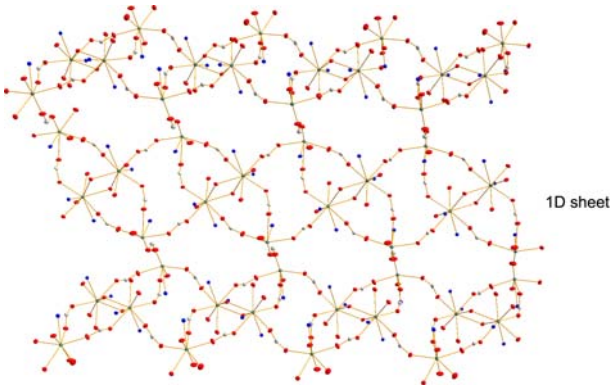

Figure 3. (a) View of 2D sheet generated by 1D chains in MOF **2**; (b) Diagrammatic drawing of 2D sheet generated by 1D chains in MOF **2**. Cyan, Sm; blue, N; red, O; gray, C.

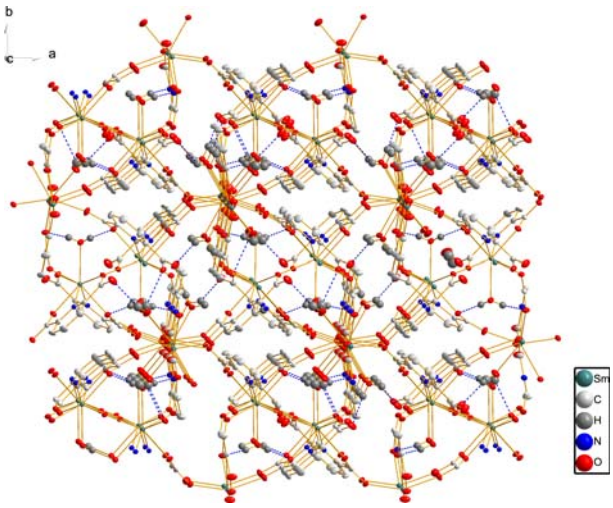

Figure 4. Hydrogen-bonding interactions in MOF **2** presenting 3D network viewed from *c*-axis direction. Cyan, Sm; blue, N; red, O; gray, C.

Luminescent Properties. Luminescence studies. It is known that the lanthanide ions are promising as luminescent probes and the lanthanide centered emission can be

Table 4. Distances (Å) and Angles (°) of Hydrogen Bonds for **1-3**

D-H···A	d (D-H)	d (H···A)	d (D···A)	∠ (D-H···A)
MOF **1**[a]				
O(4W)-H(4WB)...O(1)[#6]	0.85	1.99	2.76(2)	150.9
O(4W)-H(4WA)...O(3W)[#5]	0.85	2.07	2.83(2)	150.1
O(3W)-H(3WB)...O(2W)	0.85	2.50	2.908(7)	110.5
O(3W)-H(3WB)...O(6)[#7]	0.85	2.18	2.957(8)	151.1
O(3W)-H(3WA)...O(1)[#8]	0.85	2.49	2.914(8)	111.7
O(2W)-H(2WB)...O(5)[#4]	0.85	2.30	2.874(7)	125.3
O(2W)-H(2WA)...O(5)[#7]	0.95	1.89	2.784(7)	154.2
O(1W)-H(1WB)...O(9)	0.85	2.48	2.985(6)	119.3
O(1W)-H(1WB)...O(10)[#3]	0.85	2.05	2.893(6)	171.6
O(1W)-H(1WA)...O(7)[#1]	0.85	2.01	2.853(7)	170.6
MOF **2**[b]				
O(1W)-H(1WA)...O(11)[#4]	0.85	2.05	2.846(4)	155.8
O(1W)-H(1WB)...O(3)[#1]	0.85	1.93	2.775(4)	177.2
O(2W)-H(2WA)...O(1)[#7]	0.85	1.95	2.788(5)	167.8
O(2W)-H(2WB)...O(1)[#6]	0.85	2.24	2.982(5)	145.2
O(3W)-H(3WB)...O(4W)[#3]	0.85	2.03	2.841(15)	160.2
O(3W)-H(3WB)...O(5)[#8]	0.85	2.47	2.942(5)	116.1
O(4W)-H(4WA)...O(4W)[#9]	0.85	2.08	2.77(3)	138.8
O(4W)-H(4WB)...O(5)[#5]	0.85	2.59	2.831(16)	97.7
MOF **3**[c]				
O(4W)-H(4WB)...O(5)[#2]	0.85	2.15	2.788(12)	132.2
O(4W)-H(4WA)...O(4W)[#7]	0.85	2.03	2.86(2)	167.9
O(3W)-H(3WB)...O(4)	0.85	2.31	2.843(4)	121.4
O(3W)-H(3WA)...O(5)[#9]	0.85	2.25	2.982(5)	144.3
O(2W)-H(2WB)...O(1)[#4]	0.85	2.31	3.016(4)	141.2
O(2W)-H(2WA)...O(1)[#8]	0.85	1.99	2.794(4)	157.4
O(1W)-H(1WB)...O(3)[#1]	0.85	1.93	2.767(4)	166.0
O(1W)-H(1WA)...O(9)	0.85	2.41	2.864(4)	114.3
O(1W)-H(1WA)...O(10)[#3]	0.85	2.02	2.844(4)	162.1

[a]Symmetry transformations of **1** used to generate equivalent atoms: [#1]–x+1, –y+1, –z+1; [#3]–x+2, –y+1, –z+1; [#4]x, –y+1/2, z–1/2; [#5]x–1, y, z; [#6]x, –y+1/2, z+1/2; [#7]–x+2, y–1/2, –z+3/2; [#8]x+1, –y+1/2, z+1/2. [b]Symmetry transformations of **3** used to generate equivalent atoms: [#1]–x, –y, –z+1; [#3]x, –y+1/2, z+1/2; [#4]–x+1, –y, –z+1; [#5]x+1, y, z; [#6]x, –y+1/2, z–1/2; [#7]x+1, y+1/2, –z+3/2; [#8]x+1, –y+1/2, z+1/2; [#9]–x+2, –y, –z. [c]Symmetry transformations of **4** used to generate equivalent atoms: [#1]–x+2, –y, –z+1; [#2]x–1, y, z; [#3]–x+1, –y, –z+1; [#4]x, –y+1/2, z+1/2; [#7]–x, –y, –z+2; [#8]–x+1, y+1/2, –z+1/2; [#9]x–1, –y+1/2, z–1/2.

Table 5. Comparison of the corresponding distances (Å, average) for MOFs **1-3**

	1	**2**	**3**
Ln–O_W	2.591	2.500	2.484
Ln–O_C	2.518	2.435	2.417
Ln–N	2.673	2.567	2.538
Ln···Ln	6.619	6.488	6.463
	4.448	4.295	4.268

sensitized by molecules having the π electrons. Significant emission, characteristic of the lanthanide ions, however, can be observed by employing suitable ligands that can absorb and transfer the energy to the central lanthanide ions. Generally, in coordination MOFs, the ligand is excited to the singlet state, from where part of the energy is transferred to the triplet state through inter system crossing. When the energy levels are favorable, the triplet excited state can transfer the energy to the metal centers, resulting in metal centered luminescence.[81-83] The success of this transfer of energy is reflected in the suppressing of the intra-ligand emission in the luminescence spectra.

To examine the possibility of modifying the luminescent properties through cations exchange, the solid sample of **1** was immersed in DMF (10^{-4} M) containing metal cations to generate solutions at room temperature. Emission spectra of **1** in the presence of Mg^{2+}, Zn^{2+}, Cd^{2+}, Pb^{2+} Hg^{2+}, and Cu^{2+} ions with respect to MOF **1** are illustrated in Figure 5. The emission intensity of MOF **1** enhances gradually upon the addition of **1-3** equivalents of Mg^{2+}($Mg(CH_3COO)_2$) with respect to **1**. As the concentration of Mg^{2+} was controlled at 1 equivalent, its highest peak at 332 nm (excited at 302 nm) is nearly more than three times as intense as the corresponding peak of the solution without Mg^{2+}. When 3 equivalent of Cd^{2+} ($Cd(CH_3COO)_2$) is introduced, the emission intensity of MOF **1** increased up to three times comparing to the original MOF. To make a further understanding of this phenomenon, the same experiments were performed for the

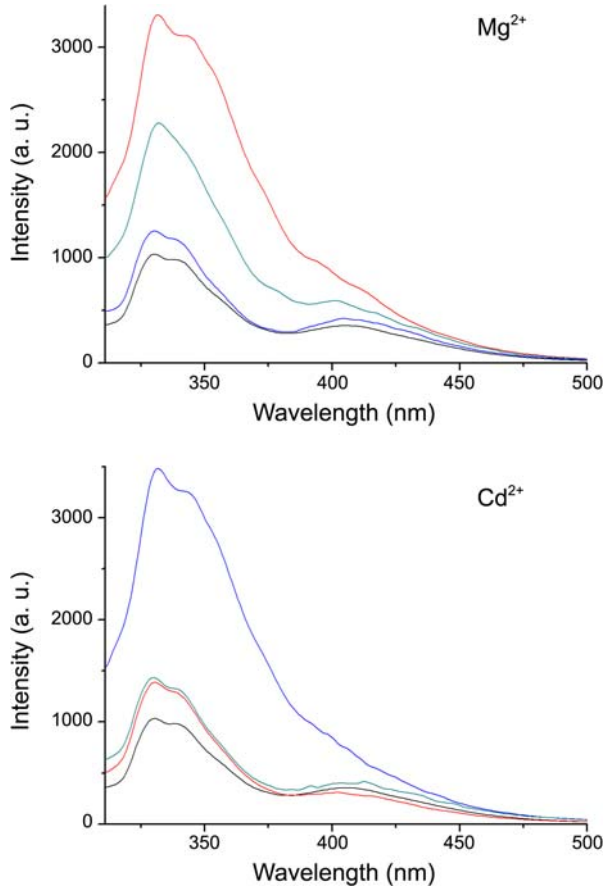

Figure 5. Emission spectra of **1** in DMF (10^{-4} M) at room temperature (excited at 302 nm) in the presence of 0-3 equiv of Mg^{2+} and Cd^{2+} ions with respect to **1**, respectively: black, no addition; red, 1 equiv; blue, 2 equiv; green, 3 equiv.

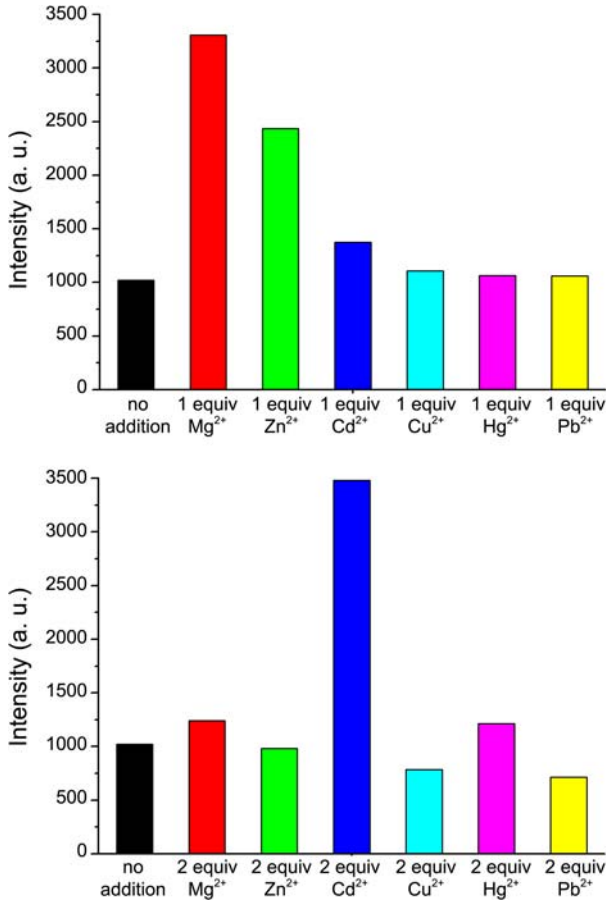

Figure 6. Different concentrations of metal ion influence the luminescent intensity of **1** at 332 nm in DMF at room temperature upon the addition of Mg^{2+}, Zn^{2+}, Cd^{2+}, Cu^{2+}, Hg^{2+}, and Pb^{2+} ions (excited at 302 nm).

introduction of Zn^{2+} ($Zn(CH_3COO)_2$), Pb^{2+} ($Pb(CH_3COO)_2$), Hg^{2+}($HgCl_2$), and Cu^{2+}($Cu(CH_3COO)_2$) into the DMF solution of MOF **1**, whereas the emission intensities just enhanced slightly (see Figure 6).

As for **2**, the solid sample was immersed in CH_3OH (10^{-4} M) containing metal cations to generate solutions at room temperature. When the introduction of Pb^{2+}($Pb(CH_3COO)_2$) is adjusted at 3 equivalent, the intensity of emission spectra at 332 and 344 nm (excited at 234 nm) sharply reduces by 23 times compared to that without adding, while the emission intensity decreases by 4 times at the presence of Cd^{2+} ion (3 equivalent, $Cd(CH_3COO)_2$) with respect to the original MOF **2**, as shown in Figure 7. Based on the observations above mentioned, the emission of MOF **2** may be due to the ligand-to-metal-charge-transfer (LMCT) from PDA^{2-} molecules to lanthanide emission centers are moderately efficient.[5,84-88] Other metal ions including Ca^{2+} and Zn^{2+} ions only make indistinctive decreases of the intensities of emission spectra of **2** (see Figure 8). Interestingly, the distinct decrease and enhancement of the emission intensities of **2** caused by Pb^{2+} and Cd^{2+} are more prominent at the concentration of 3 equivalent as compared with 1 or 2 equivalent metal ions, which is related to the stronger concentration-dependent selectivity of MOF **2** in the presence of Pb^{2+} and Cd^{2+}. The mechanism of the luminescent feature of the MOFs along with its dependence on the co-existing metal ions is still under investigation.

Thermal Analysis. Thermogravimetric analyses of **1-3** were performed in the N_2 stream from room temperature to 1000 °C. These studies are particularly informative regarding the water content of the synthesized materials and, were of great importance to help in the quantication of the water content present in the solvent accessible area of the 3D frameworks. All the lanthanide MOFs show almost similar TG and DTG curves and decompose in two steps as displayed in Figure 9. The first weight loss stage of **1-3** take place covering the temperature ranges of 106-196 °C, 110-180 °C and 112-206 °C with the observed weight losses of 7.73%, 7.56% and 7.40%, respectively, and they are close to the calculated values of 7.03% (**1**), 6.85% (**2**) and 6.74% (**3**), which correspond to the destruction of one quarter of lattice water and three coordinated water molecules, and are consistent with the crystal structure analysis. Subsequently, the TG curves undergo a stable plateau around ~200-440 °C and further decomposition processes do not occur until 444, 440 and 455 °C due to the ligands decomposition, giving the nal residual products of Ln_2O_3. Whereas the final remnants

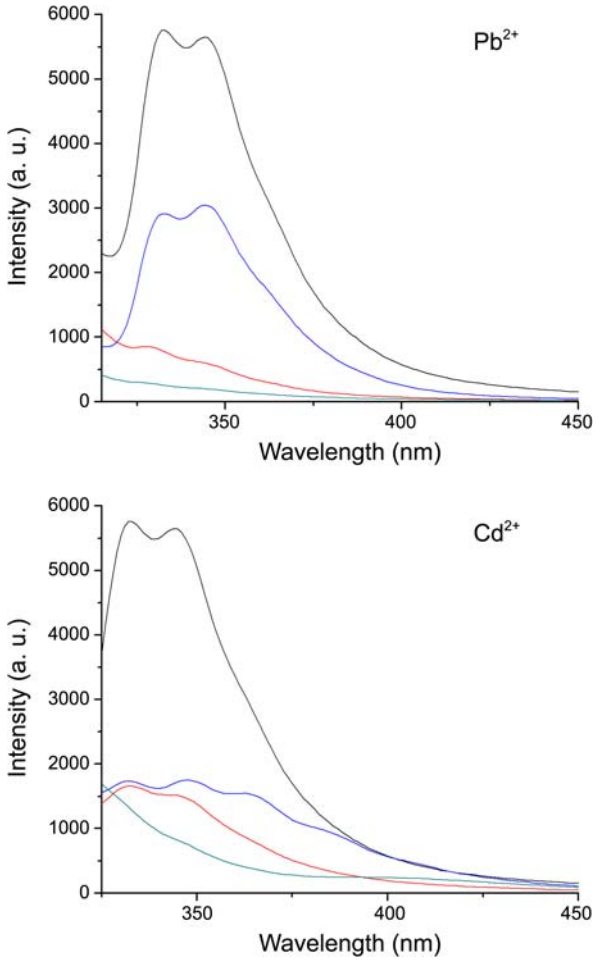

Figure 7. Emission spectra of **2** in CH_3OH (10^{-4} M) at room temperature (excited at 234 nm) in the presence of 0-3 equiv of Cd^{2+} and Pb^{2+} ions with respect to **2**, respectively: black, no addition; red, 1 equiv; blue, 2 equiv; green, 3 equiv.

of 45.70% (**1**), 38.96% (**2**) and 43.57% (**3**) suggest that **1** and **3** do not decompose completely under the experimental temperature (calculated values of La_2O_3, Nd_2O_3 and Gd_2O_3 are 39.18% (**1**), 39.73% (**2**) and 41.75% (**3**), respectively).

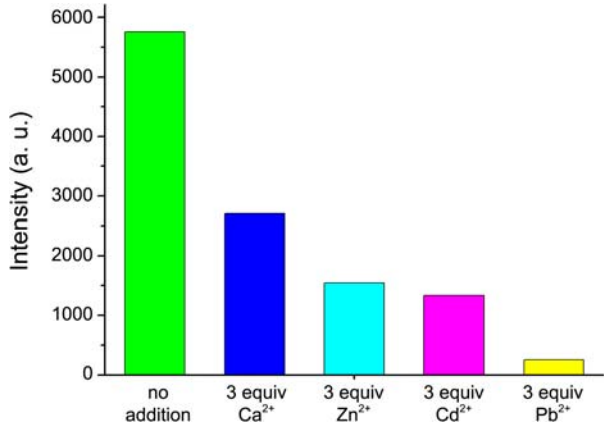

Figure 8. Different concentrations of metal ion influence the luminescent intensity of **2** at 330 nm in CH_3OH at room temperature upon the addition of Ca^{2+}, Zn^{2+}, Cd^{2+}, and Pb^{2+} ions (excited at 234 nm).

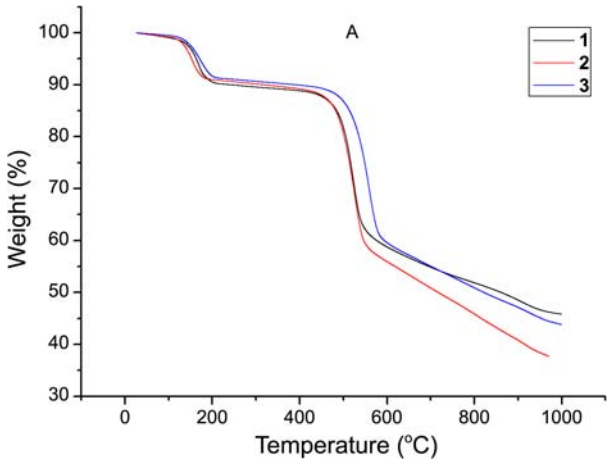

Figure 9. The TG curves for MOFs **1-3**.

Then the compounds continue to decompose above this temperature and complete decomposition do not achieved until above 1000 °C. Higher decomposing temperatures of lanthanide MOFs **1-3** represent considerable thermal stability, suggesting that high coordination number and the coordination environment of lanthanide ions with PDA^{2-} ligand have remarkably effects on the framework rigidity and thermal stability.

Conclusion

Three novel coordination polymers containing PDA^{2-} ligand and metal Ln(III) (Ln=La, Sm and Gd) centers with eight-coordinated and nine-coordinated environments have been successfully synthesized under hydrothermal condition, which are assembled into 3D supramolecular networks based on the building blocks of homometallic $Ln_4C_4O_8$ unit (16-membered ring) through O–C–O bridges and hydrogen bonds. X-ray single crystal diffraction analysis indicates that MOFs 1-3 are isomorphous and isostructural. The crystal lattice parameters such as the average distances of Ln–O_W, Ln–O_C, Ln–N and Ln···Ln in lanthanide MOFs 1-3 regularly decrease with the series of La, Nd, Sm to Gd owing to the lanthanide contraction effect. These characters also can be proofed by thermal analysis. Higher decomposing temperatures of 1-3 indicate that they are considerable stable. The luminescent properties of 1 and 2 present selectivity toward Mg^{2+}, Cd^{2+} and Pb^{2+} ions, which may be considered as selective luminescent probes for these metals. Multicarboxylate acid based sites within porous lanthanide MOFs are expected to play very important roles for their recognition of small molecules and metal ions. Further efforts will be focused on the design and assembly of lanthanide porous luminescent lanthanide MOFs with tuned micropores to enhance their recognition selectivity to induce preferential binding with respect to different metal ions, leading to highly selective luminescent MOFs probes, which might be exploited for the sensing of metal ions in the near future.

Acknowledgments. This work was supported by the

Natural Science Foundation of Henan Province, P.R. China (No. 12B150005, 122102210174 and 12B150004).

References

1. Devic, T.; Serre, C.; Audebrand, N.; Marrot, J.; Férey, G. *J. Am. Chem. Soc.* **2005**, *127*, 12788.
2. Férey, G.; Mellot-Draznieks, C.; Serre, C.; Millange, F.; Dutour, J.; Surble, S.; Margiolaki, I. *Science* **2005**, *309*, 2040.
3. Shi, F.; Cunha-Silva, L.; Ferreira, R. A. S.; Mafra, L.; Trindade, T.; Carlos, L.; Paz, F. A. A.; Rocha, J. *J. Am. Chem. Soc.* **2008**, *130*, 150.
4. Aillaud, I.; Collin, J.; Duhayon, C.; Guillot, R.; Lyubov, D.; Schulz, E.; Trifonov, A. *Chem. Eur. J.* **2008**, *14*, 2189.
5. Chen, B. L.; Wang, L. B.; Xiao, Y. Q.; Fronczek, F. R.; Xue, M.; Cui, Y. J.; Qian, G. D. *Angew. Chem. Int. Ed.* **2009**, *48*, 500.
6. Tranchemontagne, D. J.; Mendoza-Cortes, J. L.; Keee, M. O'; Yaghi, O. M. *Chem. Soc. Rev.* **2009**, *38*, 1257.
7. Ockwig, N. W.; Delgado-Friedrichs, O.; Keeffe, M. O'; Yaghi, O. M. *Acc. Chem. Res.* **2005**, *38*, 176.
8. Millward, A. R.; Yaghi, O. M. *J. Am. Chem. Soc.* **2005**, *127*, 17998.
9. Côté, A. P.; Benin, A. I.; Ockwig, N. W.; O'Keeffe, M.; Matzger, A. J.; Yaghi, O. M. *Science* **2005**, *310*, 1166.
10. Yaghi, O. M.; O'Keeffe, M.; Ockwig, N. W.; Chae, H. K.; Eddaoudi, M.; Kim, J. *Nature* **2003**, *423*, 705.
11. Chae, H. K.; Siberio-Pérez, D. Y.; Kim, J.; Go, Y. B.; Eddaoudi, M.; Matzger, A. J.; O'Keeffe, M.; Yaghi, O. M. *Nature* **2004**, *427*, 523.
12. Chen, B. L.; Eddaoudi, M.; Hyde, S. T.; O'Keeffe, M.; Yaghi, O. M. *Science* **2001**, *291*, 1021.
13. Eddaoudi, M.; Kim, J.; Rosi, N.; Vodak, D.; Wachter, J.; O'Keeffe, M.; Yaghi, O. M. *Science* **2002**, *295*, 469.
14. Suh, M. P.; Cheon, Y. E.; Lee, E. Y. *Coord. Chem. Rev.* **2008**, *252*, 1007.
15. Rieter, W. J.; Pott, K. M.; Taylor, K. M. L.; Lin, W. J. *Am. Chem. Soc.* **2008**, *130*, 11584.
16. Latroche, M.; Surblé, S.; Serre, C.; MellotDraznieks, C.; Llewellyn, P. L.; Lee, J. H.; Chang, J. S.; Jhung, S. H.; Férey, G. *Angew. Chem. Int. Ed.* **2006**, *45*, 8227.
17. Halder, G. J.; Kepert, C. J.; Moubaraki, B.; Murray, K. S.; Cashion, J. D. *Science* **2002**, *298*, 1762.
18. Férey G. *Chem. Soc. Rev.* **2007**, *37*, 191.
19. Guo, J.; Zhang, J.; Zhang, T.; Wu, R.; Yu, W. *Act. Phys. Chim. Sin.* **2006**, *22*, 1206.
20. Harbuzaru, B. V.; Corma, A.; Rey, F.; Atienzar, P.; Jordá, J. L.; García, H.; Ananias, D.; Carlos, L. D.; Rocha, J. *Angew. Chem. Int. Ed.* **2008**, *47*, 1080.
21. Dybtsev, D. N.; Nuzhdin, A. L.; Chun, H.; Bryliakov, K. P.; Talsi, E. P.; Fedin, V. P.; Kim, K. *Angew. Chem. Int. Ed.* **2006**, *45*, 916.
22. Chen, B.; Wang, L.; Zapata, F.; Qian, G.; Lobkovsky, E. B. *J. Am. Chem. Soc.* **2008**, *130*, 6718.
23. Hasegawa, S.; Horike, S.; Matsuda, R.; Furukawa, S.; Mochizuki, K.; Kinoshita, Y.; Kitagawa, S. *J. Am. Chem. Soc.* **2007**, *129*, 2607.
24. Horike, S.; Bureekaew, S.; Kitagawa, S. *Chem. Commun.* **2008**, 471.
25. Jia, J. H.; Lin, X.; Wilson, C.; Blake, A. J.; Champness, N. R.; Hubberstey, P.; Walker, G.; Cussen, E. J.; Schroder, M. *Chem. Commun.* **2007**, 840.
26. Chen, B.; Zhao, X.; Putkham, A.; Hong, K.; Lobkovsky, E. B.; Hurtado, E. J.; Fletcher, A. J.; Thomas, K. M. *J. Am. Chem. Soc.* **2008**, *130*, 6411.
27. Zhang, J. P.; Chen, X. M. *J. Am. Chem. Soc.* **2008**, *130*, 6010.
28. Ma, S.; Wang, X. S.; Yuan, D.; Zhou, H. C. *Angew. Chem. Int. Ed.* **2008**, *120*, 4198.
29. Dinc, M.; Long, J. R. *Angew. Chem. Int. Ed.* **2008**, *120*, 6870.
30. Kurmoo, M. *Chem. Soc. Rev.* **2009**, *38*, 1353.
31. Yang, S.; Lin, X.; Blake, A. J.; Thomas, K. M.; Hubberstey, P.; Champness, N. R.; Schröder, M. *Chem. Comm.* **2008**, *46*, 6108.
32. Dong, Y. B.; Wang, P.; Ma, J. P.; Zhao, X. X.; Wang, H. Y.; Tang, B.; Huang, R. Q. *J. Am. Chem. Soc.* **2007**, *129*, 4872.
33. Morris, R. E.; Wheatley, P. S. *Angew. Chem. Int. Ed.* **2008**, *47*, 4966.
34. Halim, M.; Tremblay, M. S.; Jockusch, S.; Turro, N. J.; Sames, D. *J. Am. Chem. Soc.* **2007**, *129*, 7704.
35. Davis, M. E. *Nature* **2002**, *417*, 813.
36. Lee, J. Y.; Farha, O. K.; Roberts, J.; Scheidt, K. A.; Nguyen, S. B. T.; Hupp, J. T. *Chem. Soc. Rev.* **2009**, *38*, 1450.
37. Feng, M. L.; Kong, D. N.; Xie, Z. L.; Huang, X. Y. *Angew. Chem. Int. Ed.* **2008**, *120*, 8751.
38. Allendorf, M.; Bauer, C.; Bhakta, R.; Houk, R. *Chem. Soc. Rev.* **2009**, *38*, 1330.
39. Wang, P.; Ma, J. P.; Dong, Y. B.; Huang, R. Q. *J. Am. Chem. Soc.* **2007**, *129*, 10620.
40. Li, J. R.; Kuppler, R. J.; Zhou, H. C. *Chem. Soc. Rev.* **2009**, *38*, 1477.
41. Manos, M. J.; Malliakas, C. D.; Kanatzidis, M. G. *Chem. Eur. J.* **2007**, *13*, 51.
42. Feng, M. L.; Kong, D. N.; Xie, Z. L.; Huang, X. Y. *Angew. Chem. Int. Ed.* **2008**, *47*, 8623.
43. Bunzli, J. C. G.; Piguet, C. *Chem. Soc. Rev.* **2005**, *34*, 1048.
44. Bunzli, J. C. G. *Acc. Chem. Res.* **2006**, *39*, 53.
45. Lu, W. G.; Jiang, L.; Feng, X. L.; Lu, T. B. *Inorg. Chem.* **2009**, *48*, 6997.
46. Lowe, M. P.; Parker, D. *Chem. Commun.* **2000**, 707.
47. Liu, W. S.; Jiao, T. Q.; Li, Y. Z.; Liu, Q. Z.; Tan, M. Y.; Wang, H.; Wang, L. F. *J. Am. Chem. Soc.* **2004**, *126*, 2280.
48. Zhao, B.; Chen, X. Y.; Cheng, P.; Liao, D. Z.; Yan, S. P.; Jiang, Z. H. J. *Am. Chem. Soc.* **2004**, *126*, 15394.
49. Zhu, Q. L.; Sheng, T. L.; Fu, R. B.; Hu, S. M.; Chen, J. S.; Xiang, S. C.; Shen, C. J.; Wu, X. T. *Cryst. Growth Des.* **2008**, *9*, 5128.
50. Zhu, T.; Ikarashi, K.; Ishigaki, T.; Uematsu, K.; Toda, K.; Okawa, H.; Sato, M. *Inorg. Chim. Acta* **2009**, *362*, 3407.
51. Wang, Z. Q.; Cohen, S. M. *Chem. Soc. Rev.* **2009**, *38*, 1315.
52. Custelcean, R.; Gorbunova, M. G. *J. Am. Chem. Soc.* **2005**, *127*, 16362.
53. Prasad, T. K.; Rajasekharan, M. V. *Cryst. Growth Des.* **2006**, *6*, 488.
54. Cabarrecq, C. B.; Ghys, J. D.; Fernandes, A.; Jaud, J.; Trombem, J. C. *Inorg. Chim. Acta* **2008**, *361*, 2909.
55. Mahata, P.; Ramya, K. V.; Natarajan, S. *Dalton Trans.* **2007**, *36*, 3973.
56. Marcelo, O.; Rodrigues, Nivan B.; Júnior, D. C.; Carlos, A.; Simone, D.; Adriano, A. S.; Araújo; Brito-Silva, A. M.; Filipe, A.; Almeida, P.; Maria, E.; Mesquita, D.; Severino, A.; Júnior, Ricardo, O. F. J. *Phys. Chem. B* **2008**, *112*, 4204.
57. Liu, M. S.; Yu, Q. Y.; Cai, Y. P.; Su, C. Y.; Lin, X. M.; Zhou, X. X.; Cai, J. W. *Cryst. Growth Des.* **2008**, *8*, 4083.
58. Leonard, J. P.; Jensen, P.; McCabe, T.; O'Brien, J. E.; Peacock, R. D.; Kruger, P. E.; Gunnlaugsson, T. *J. Am. Chem. Soc.* **2007**, *129*, 10986.
59. Cai, M. G.; Chen, J. D.; Taha, M. *Inorg. Chem. Commun.* **2010**, *13*, 199.
60. Dos Santos, C. M. G.; Harte, A. J.; Quinn, S. J.; Gunnlaugsson, T. *Coordin. Chem. Rev.* **2008**, *252*, 2512.
61. Feng, X.; Shi, X. G.; Sun, Q.; Wang, L. Y.; Zhao, J. S.; Liu, Y. Y. *Synth. React. Inorg. Met.-Org. Chem.* **2010**, *40*, 479.
62. Huang, Y. G.; Yuan, D. Q.; Gong, Y. Q.; Jiang, F. L.; Hong, M. C. *J. Mol. Struct.* **2008**, *872*, 99.
63. Yang, L. R.; Song, S.; Shao, C. Y.; Zhang, W.; Zhang, H. M.; Bu, Z. W.; Ren, T. G. *Synth. Met.* **2011**, *161*, 925.
64. Yang, L. R.; Song, S.; Shao, C. Y.; Zhang, W.; Zhang, H. M.; Bu, Z. W.; Ren, T. G. *Synth. Met.* **2011**, *161*, 1500.
65. Sheldrick, G. M. SADABS: Empirical Absorption Correction

Software, University of Göttingen, Institut fur Anorganische Chemieder Universitat, Tammanstrasse 4, D-3400 Göttingen, Germany, 1999.
66. Sheldrick, G. M. SHELXTL: version 5. Reference manual, Siemens Analytical X-ray Systems, USA, 1996.
67. Tang, R. R.; Gu, G. L.; Zhao, Q. G. *Spectrochim. Acta A* **2008**, *71*, 371.
68. Nakamoto, K. *Infrared and Raman Spectra of Inorganic and Coordination Compounds*; John Wiley and Sons: New York, 1997.
69. Yang, L. R.; Song, S.; Zhang, H. M.; Zhang, W.; Bu, Z. W.; Ren, T. G. *Synth. Met.* **2011**, *161*, 2230.
70. Tancrez, N.; Feuvrie, C.; Ledoux, I.; Zyss, J.; Toupet, L.; Le Bozec, H.; Maury, O. *J. Am. Chem. Soc.* **2005**, *127*, 13474.
71. Shi, F. N.; Cunha-Silva, L.; Trindade, T.; Paz, F. A. A.; Rocha, J. *Cryst. Growth Des.* **2009**, *9*, 2098.
72. Aghabozorg, H.; Moghimi, A.; Manteghi, F.; Ranjbar, M. Z. *Anorg. Allg. Chem.* **2005**, *631*, 909.
73. Zhao, B.; Yi, L.; Dai, Y.; Chen, X. Y.; Cheng, P.; Liao, D. Z.; Yan, S. P.; Jiang, Z. H. *Inorg. Chem.* **2005**, 911.
74. Brouca-Cabarrecq, C.; Fernandes, A.; Jaud, J.; Costes, J. *Inorg. Chim. Acta* **2002**, *332*, 54.
75. Ghosh, S. K.; Bharadwaj, P. K. *Inorg. Chem*. **2004**, *43*, 2293.
76. Gao, H. L.; Yi, L.; Zhao, B.; Zhao, X. Q.; Cheng, P.; Liao, D. Z.; Yan, S. P. *Inorg. Chem.* **2006**, *45*, 5980.
77. Song, Y.; Niu, Y.; Hou, H.; Zhu, Y. *J. Mol. Struct.* **2004**, *689*, 69.
78. Ghosh, S. K.; Bharadwaj, P. K. *Inorg. Chem.* **2005**, *44*, 3156.
79. Yao, J.; Deng, B.; Sherry, L. J.; McFarland, A. D.; Ellis, D. E.; Van Duyne, R. P.; Ibers, J. A. *Inorg. Chem.* **2004**, *43*, 7735.
80. Gao, H. L.; Yi, L.; Zhao, B.; Zhao, X. Q.; Cheng, P.; Liao, D. Z.; Yan, S. P. *Inorg. Chem.* **2006**, *45*, 5980.
81. Armelao, L.; Quici, S.; Barigelletti, F.; Accorsi, G.; Bottaro, G.; Cavazzini, M.; Tondello, E. *Coord. Chem. Rev.* **2010**, *254*, 487.
82. Chandler, B. D.; Cramb, D. T.; Shimizu, G. K. H. *J. Am. Chem. Soc.* **2006**, *128*, 10403.
83. Selvin, P. R. *Nat. Struct. Biol*. **2000**, *7*, 730.
84. Mahata, P.; Ramya, K. V.; Natarajan, S. *Dalton Trans*. **2007**, *36*, 3973.
85. Yin, H.; Liu, S. X. *J. Mol. Struct*. **2009**, *918*, 165.
86. Arnaud, N.; Vaquer, E.; Georges, J. *J. Analyst.* **1998**, *123*, 261.
87. Reineke, T. M.; Eddaoudi, M.; Fehr, M.; Kelley, D.; Yaghi, O. M. *J. Am. Chem. Soc.* **1999**, *121*, 1651.
88. Lu, W. G.; Jiang, L.; Feng, X. L.; Lu, T. B. *Inorg. Chem.* **2009**, *48*, 6997.